Published in final edited form as:
Biochemistry. 2010 February 9; 49(5): 912. doi:10.1021/bi9021186.

Investigation of Anticapsin Biosynthesis Reveals a Four-Enzyme Pathway to Tetrahydrotyrosine in *Bacillus subtilis*†

Sarah A. Mahlstedt and **Christopher T. Walsh***
Department of Biological Chemistry and Molecular Pharmacology, Harvard Medical School, Boston, MA 02115

Abstract

Bacillus subtilis produces the antibiotic anticapsin as an L-Ala-L-anticapsin dipeptide precursor known as bacilysin, whose synthesis is encoded by the *bacA-D* genes and the adjacent *ywfGH* genes. To evaluate the biosynthesis of the epoxycyclohexanone amino acid anticapsin from the primary metabolite prephenate we have overproduced, purified and characterized the activity of the BacA, BacB, YwfH, and YwfG proteins. BacA is an unusual prephenate decarboxylase that avoids the typical aromatization of the cyclohexadienol ring by protonating C_8 to produce an isomerized structure. BacB then catalyzes an allylic isomerization, generating a conjugated dienone with a 295 nm chromophore. Both the BacA and BacB products are regioisomers of H_2HPP (dihydro-4-hydroxyphenylpyruvate). The BacB product is then a substrate for the short chain reductase YwfH which catalyzes the conjugate addition of hydride at the C_4 olefinic terminus using NADH to yield the cyclohexenol- containing tetrahydro-4-hydroxyphenylpyruvate H_4HPP. In turn this keto acid is a substrate for YwfG, which promotes transamination (with L-Phe as amino donor), to form tetrahydrotyrosine (H_4Tyr). Thus BacA, BacB, YwfH and YwfG act in sequence in a four enzyme pathway to make H_4Tyr, which has not previously been identified in *B. subtilis* but is a recognized building block in cyanobacterial nonribosomal peptides such as micropeptins and aeruginopeptins.

Bacillus subtilis produces a variety of polyketide and peptide-derived antibiotics, such as difficidin, bacillaene, mycosubtilin, fengycin, and surfactin (1). Bacilysin (**1**), a deceptively simple example of a *B. subtilis* antibiotic (Figure 1a), was first isolated in 1946 (2). Its structure was solved in 1970 (3), though corrections to its assigned stereochemistry were made decades later (4,5). Over the years this compound has been referred to by a variety of names, including bacillin and tetaine (6,7), and has been identified in other *Bacillus* species (8-10). Bacilysin is a dipeptide consisting of an N-terminal alanine residue linked to a non-proteinogenic epoxycyclohexanone-containing amino acid referred to as anticapsin (**2**). This unusual residue is the key to bacilysin's antibiotic and antifungal activity (11). The dipeptide is exported by producing cells and can be taken up by a competitor via di- to oligopeptide uptake systems (12,13). Cytoplasmic peptidases cleave the dipeptide, releasing the anticapsin warhead (11, 14). Anticapsin can then bind to the active site of the cell wall biosynthetic enzyme glucosamine-6-phosphate synthase as a mimic of the natural glutamine substrate, resulting in irreversible inhibition of the enzyme. Covalent attachment of anticapsin presumably arises from the reaction of an active site cysteine thiol with the epoxide functional group (14,15).

The biosynthesis of anticapsin by *B. subtilis* has remained a mystery in the six decades since its isolation. Originally it was suspected that the amino acid was derived from either tyrosine

†This work was supported in part by the National Institutes of Health GM 49338 (CTW) and the National Science Foundation Graduate Research Fellowship Program (SAM).

*To whom correspondence should be addressed: christopher_walsh@hms.harvard.edu, phone: 617.432.1715, fax: (+1)617.432.0483

or phenylalanine. However, radioactive isotope labeling studies indicated that neither of these compounds were the anticapsin precursors (16). *B. subtilis* cells fed radiolabeled shikimate produced labeled bacilysin (16), indicating that the precursor must be an intermediate along the aromatic amino acid biosynthetic pathway. Several years later genetic knockout studies narrowed down the possible precursors (17). Bacteria typically produce Tyr and Phe by first converting chorismate to prephenate through the action of chorismate mutase. Prephenate is then decarboxylated and aromatized to form either phenylpyruvate (prephenate dehydratase) or 4-hydroxyphenylpyruvate (prephenate dehydrogenase), which can be transaminated to produce Phe and Tyr, respectively. Mutations in prephenate dehydratase and prephenate dehydrogenase, the enzymes that catalyze decarboxylation, did not halt production of bacilysin, so it was concluded that anticapsin must be derived from prephenate **3** (17).

The gene cluster encoding bacilysin biosynthesis (Figure 1c) has been identified and sequenced (10, 18), though there has been some dispute as to the boundaries of the cluster and whether it contains all of the genes necessary for bacilysin production. Most discussions of the biosynthetic pathway state that the cluster contains five genes, which were historically referred to as *ywfB-F*, but have been renamed *bacA-E* to denote their relevance to bacilysin formation. The products of the first three genes are known to be critical for formation of anticapsin (10). The fourth gene, *bacD*, encodes an L-amino acid ligase that has been previously characterized *in vitro* and shown to have promiscuous activity (19). It follows that the BacD enzyme catalyzes amide bond formation between Ala and anticapsin. The fifth gene, *bacE*, is involved in host resistance (10). Intriguingly, upon closer inspection of the gene cluster one finds a sixth ORF, *ywfG*, which generally is not annotated with the rest of the cluster. Additionally, a separate, monocistronic gene, *ywfH*, located immediately downstream of the bacilysin gene cluster, has been reported to be important in the production of bacilysin (18).

Bioinformatic analysis has led to the assignment of possible activies for each of the seven proteins BacA-E and YwfG-H (SI Table S1). The three proteins known genetically to be involved in formation of anticapsin have the following putative functions: BacA is homologous to prephenate dehydratases, which are involved in decarboxylation of prephenate in the aromatic amino acid biosynthesis pathway; BacB is a member of the bicupin iron enzyme family; and BacC is proposed to have nicotinamide-dependent reductase or dehydrogenase activity. The protein encoded by the sixth gene *ywfG* is homologous to aminotransferases. YwfH has putative nicotinamide-dependent reductase or dehydrogenase activity.

In this work we have begun an investigation into how these enzymes can convert either prephenate or its amino acid counterpart arogenate into anticapsin (Scheme 1). The five enzymes BacA, B, C and YwfG and H have been expressed in *E. coli* and purified. While anticapsin production has yet to be reconstituted *in vitro*, four of these enzymes, BacA, BacB, YwfH and YwfG, have been found to produce a distinct non-proteinogenic amino acid, tetrahydrotyrosine (H_4Tyr) that, *inter alia*, gives insights into the novel functions of BacA.

MATERIALS AND METHODS

Bacterial Strains, Plasmids, Materials, and Instrumentation

Chemicals, including prephenic acid barium salt, were purchased from Sigma-Aldrich. NMR solvents were obtained from Cambridge Isotopes. DNA primers were synthesized by Integrated DNA Technologies. Genes were cloned from *Bacillus subtilis* sp. 168 genomic DNA purchased from ATCC. Pfu Turbo DNA Polymerase was obtained from Stratagene. Restriction enzymes and T4 DNA Ligase were purchased from New England Biolabs. The pET-28b vector was purchased from Novagen. Competent cells (TOP10 *E. coli* and BL21(DE3) *E. coli*) were purchased from Invitrogen. Plasmid and oligonucleotide purification was carried out using kits sold by Qiagen. DNA sequencing was performed by the Molecular Biology Core Facilities at

the Dana Farber Cancer Institute (Boston, MA). Nickel-nitrilotriacetic acid agarose (NiNTA) resin was purchased from Qiagen. SDS-PAGE gels were produced by Biorad. Protein was concentrated using Amicon Ultra 10 kDa MWCO filters from Millipore. Enzyme reactions were quenched by filtration to remove protein using Millipore Biomax 10 kDa MWCO centrifugal filter devices. Protein concentration was determined using a Coomassie Plus Kit from Pierce with BSA as a standard. Phenomenex Strata SCX (55 μm, 70Å) ion exchange columns were used for amino acid purification.

^{1}H and two-dimensional NMR spectra were recorded on a Varian Inova 600 MHz spectrometer at the Harvard Medical School East Quad facility. ^{13}C NMR spectra were recorded on a Varian Inova 500 MHz spectrometer at the Harvard University Chemistry Department facility. High-resolution LC-MS data was collected on an Agilent 6520 Accurate-Mass Q-TOF Mass Spectrometer fitted with an electrospray ionization (ESI) source. Analytical reverse-phase HPLC was performed on a Beckman Coulter System Gold instrument (126 solvent module, 168 detector). The 100 × 2.1 mm 5 μm Hypercarb column used for analytical HPLC was acquired from Thermo Scientific.

Cloning, Expression, and Purification of BacABC, YwfGH

Genes encoding BacABC and YwfGH were PCR amplified out of *B. subtilis* sp. 168 genomic DNA. Primers for *bacA* (5′-AAGGTCATATGATTATATTGGATAATAGCATTC-3′ and 5′-AATTCTCGAGTTAGTTTTCATCATCAACGTC-3) encoded restriction sites for enzymes Nde1 and Xho1, respectively (underlined). Primers for *bacB* (5′-AATCCGGATCCATGAAAACTAAAGAAGATATGC-3′ and 5′-AATTCTCGAGTCATTCATCCGCCTTCAT-3′) encoded restriction sites for BamH1 and Xho1, respectively. Primers for *bacC* (5′-AATCCGGATCCATGATCATGAACCTCACC-3′ and 5′-AATTCTCGAGCTATTGTGCGGTGTATCCTCC-3′) encoded restriction sites for BamH1 and Xho1. *ywfG* primers (5′-AATTCGCATATGGAAATAACACCGTCCGATGTC-3′ and 5′-AATTGGCTCGAGTTAGCGGGATGTTTCTTGTAATGACC-3′) encoded sites for Nde1 and Xho1. Primers for *ywfH* (5′-AAGGTCATATGTCAAAACGAACCGCATTTG-3′ and 5′-AATTCTCGAGTTATATGCTTTTCATGCTGC-3′) encoded Nde1 and Xho1 restriction sites. The amplified genes were ligated into plasmid pET-28b and transformed into TOP10 chemically competent *E. coli*. DNA sequencing of the purified vector confirmed gene insertion. The plasmid was then transformed into BL21(DE3) *E. coli* cells. Cultures of BL21 expression cells were grown at 37°C in Luria broth media supplemented with kanamycin (50 μg/mL) until the OD_{600} was approximately 0.4. The temperature was then reduced to 15°C (for BacB and YwfG expression), 20°C (for BacA and YwfH expression), or 25°C (for BacC expression). Once cooled the cultures were induced with 60 μM IPTG and grown overnight. Cells were harvested by centrifugation at 5000 g for 8 minutes. Pelleted cells were resuspended in lysis buffer (50 mM potassium phosphate pH 8, 150 mM NaCl) and lysed by three passes at 5000–10000 psi in an Avestin EmulsiFlex-C5 high-pressure homogenizer. The lysate was clarified by centrifugation at 35,000 g for 35 minutes. The proteins were purified out of the lysis supernatant by NiNTA affinity chromatography. Lysate was incubated with NiNTA resin for two hours at 4°C, then the resin was washed once with lysis buffer and once with lysis buffer supplemented with 5 mM imidazole. The resin was loaded to a low-pressure column and the protein eluted with a stepwise gradient of 20 mM, 40 mM, 60 mM and 200 mM imidazole in lysis buffer. Fractions containing protein were identified by SDS-PAGE and either dialyzed in lysis buffer, with or without 10% glycerol, or subjected to further purification by gel filtration on a Sephadex 200 26/60 HiLoad column with an Amersham Pharmacia Biotech AKTA FPLC system. Aliquots of protein were frozen at −80°C.

HPLC Activity Assays

Prior to assays barium prephenate was converted to potassium prephenate by five-minute incubation of a buffered prephenate solution with a twofold molar excess of potassium sulfate at room temperature (20). Barium sulfate readily precipitated and was removed from solution by centrifugation.

All assays contained 50 mM potassium phosphate pH 8 as buffer and 2 mM prephenate in 100 μL total volume. Assays were performed with varying combinations of enzymes. Cosubstrates were included in reactions when necessary at two-fold excess over substrate. YwfH required NADH as a cofactor, while YwfG required Phe. YwfG reactions also contained five-fold excess PLP to protein concentration. Reactions were quenched by removal of enzyme by filtration. Sixty μL of the quenched reaction mixture (0.12 μmol substrate) was mixed with 20 μL of OPA mixture (freshly prepared with 10 mg phthaldialdehyde, 200 μL methanol, 19.6 μL 3-mercaptopropionic acid, 880 μL 0.4 M borate buffer pH 10.4) immediately prior to injection on a Hypercarb column. Solvent A (0.1M triethylammonium acetate (TEAA)) was run at 0.5 mL/min for 3 minutes followed by a gradient from 0% to 100% B (acetonitrile) over 60 minutes, then a 5 minute wash in 100% B.

Structural Elucidation of BacA Product 4

The BacA reaction was scaled up to enable structural characterization of the transient A_{258} species **4**. It was found that **4** readily decomposed to **5** (see below) during lyophilization, thus the BacA reaction was run in D_2O to permit rapid NMR analysis. Reactions were set up with 40 mM potassium phosphate pH 8, 15.8 mM prephenate, and 2 μM BacA (buffer exchanged into 50 mM potassium phosphate pH 8, 95% D_2O) in a total volume of 700 μL (95.7% D_2O). After a 2.5 hour incubation at room temperature the reactions were quenched by filtration and analyzed by ^1H, gCOSY, and gHSQC NMR with presaturation conditions.

NMR Studies of the BacA Reaction and Subsequent Product Isomerization

The BacA reaction was studied by real-time NMR. To enable this an NMR sample was prepared with 40 mM potassium phosphate pH 8 and 15.8 mM prephenate (95.6% D_2O; 700 μL total volume). Presaturation conditions were obtained for this sample. 1 μM BacA (exchanged into 50 mM potassium phosphate pH 8, 95% D_2O) was mixed with the sample and ^1H NMR spectra were obtained every six minutes for 12 hours.

Structural Elucidation of BacB Product = the nonenzymatically rearranged BacA product

The reaction of prephenate with BacA and the susbequent nonenzymatic isomerization of this product was scaled up to produce sufficient material for NMR analysis. Reactions contained 50 mM potassium phosphate pH 8, 9.9 mM prephenate, and 20 μM BacA, prepared in glycerol-free buffer, in a total volume of 500 μL. Overnight incubations at room temperature were quenched by filtration. Filter devices were pre-rinsed once with 0.1 M NaOH and twice with water to remove traces of glycerol. Reactions were analyzed by HPLC using methods described above to verify product formation before lyophilization. The reaction products from three individually run reactions were combined in D_2O and ^1H, ^{13}C, gCOSY, gHSQC and gHMBC spectra were collected. High resolution LC-MS data were collected in negative ion mode.

The ^1H NMR of the product produced by BacA and BacB action was compared to the ^1H NMR of the non-enzymatically produced product. An NMR sample of the BacB produced product was prepared by incubation of 5 μM BacA and 5 μM BacB with 22 mM prephenate in 50 mM potassium phosphate pH 8 in a total volume of 500 μL. Reactions were quenched by filtration following an overnight incubation at room temperature. The product was lyophilized and ^1H NMR spectra obtained in D_2O. Identical reactions were performed in D_2O to assess deuterium

incorporation during the course of the reaction. High resolution LC-MS data were collected in negative ion mode on reactions run in H_2O and D_2O.

NMR Studies of the BacB Reaction

Real-time NMR data was collected for conversion of **4** to **5** by BacB. Substrate H_2HPP **4** was produced as described above. After filtration of the reaction to remove BacA, 200 nM BacB (exchanged into 50 mM potassium phosphate pH 8, 95% D_2O) was mixed with the sample and ^{1}H NMR spectra obtained every 6 minutes for 3.5 hours.

Kinetic Characterization of BacA

The extinction coefficient of H_2HPP **4** was calculated by performing endpoint assays with BacA and prephenate. An accurate prephenate concentration was determined by utilizing *E. coli* prephenate dehydratase to convert prephenate to phenylpyruvate through a previously published assay (21). The concentration of phenylpyruvate in 1 N NaOH was calculated using the known extinction coefficient of 17500 M^{-1} cm^{-1} (22). The concentration of prephenate starting material was assumed to be equal to the concentration of phenylpyruvate after the prephenate dehydratase reaction had run to completion. BacA at a 100 nM concentration was incubated with 50 μM and 100 μM prephenate while monitored at 258 nm until the reactions reached an endpoint. The absorbance of the reaction at completion was utilized to calculate the extinction coefficient of the A_{258} species to be 2900 M^{-1} cm^{-1}.

To calculate kinetic constants BacA at 100 nM concentration was incubated with varying prephenate concentrations and scans over wavelengths 220 – 340 nm were collected every 30 seconds (402 nm/min, 0.67 nm interval). Reactions were baseline corrected for prephenate absorbance over this wavelength range. A linear increase in A_{258} was observed and used to calculate the rate of product formation. These rates were fit to a Michaelis-Menton curve and K_m and k_{cat} values abstracted using the program Kaleidagraph V4.03 (Synergy Software).

UV/Vis Analysis of the BacB Reaction

When BacB was included in kinetic studies with BacA (100 nM BacA, 100 nM BacB, 50 μM prephenate) an A_{295} species (**5**) was rapidly obtained, and the A_{258} product (**4**) observed previously did not build up. The extinction coefficient of this A_{295} product was obtained by endpoint assay. 100 nM BacB and 100 nM BacA were incubated with 50 μM and 100 μM prephenate (250 μL total volume), and scans over wavelengths 220 – 340 nm were taken every 30 seconds until an endpoint was reached. The absorbance at completion was used to calculate the extinction coefficient of the A_{295} species to be 15300 ± 200 M^{-1} cm^{-1}.

Rate of 4 decomposition to 5

To determine whether decomposition of the A_{258} species (**4**) to an A_{295} species (**5**) was catalyzed by BacA, the rate of formation of **5** was monitored in the presence and absence of BacA. H_2HPP **4** was produced by incubating 200 μM prephenate with 100 nM BacA in 50 mM potassium phosphate pH 8 (500 μL total volume) for 20 minutes, followed by filtration to quench the reaction. Half of the filtrate was monitored over 20 minutes over a 220-340 nm wavelength range to assess formation of **5** at 295 nm. BacA was added to 100 nM final concentration to the other half of the reaction and the rate of formation of **5** monitored. A linear increase in A_{295} was observed for both samples and used to calculate the rate of **5** formation.

Structural Elucidation of YwfG Product

A series of sequential incubations were run to collect enough sample of the YwfG reaction product for NMR analysis. First, four BacA reactions were run under the conditions and scale described above for formation of H_2HPP **5** in a total volume of 500 μL, with the substitution

of the volatile TEAA buffer (50 mM, pH 8) for phosphate. The reactions were quenched by filtration and lyophilized following analysis of the reactions by HPLC. Subsequently, four large-scale YwfH reactions were run by dissolving the product of each BacA reaction in water and mixing the solutions with 50 mM TEAA pH 8, 20 mM NADH, and 30 μM YwfH in 500 μL final volume. Reactions were left at room temperature overnight, quenched by filtration, and analyzed by HPLC prior to lyophilization. Samples of the YwfH reaction were analyzed by high-resolution LC/MS in negative ion mode, ^{1}H NMR, and gCOSY NMR. YwfG reactions were set up by dissolving the product of each YwfH reaction in water and incubating the solution with 30 μM YwfG, 20 mM Phe and 0.1 mM PLP in 50 mM TEAA pH 8 (500 μL total volume). Analytical HPLC confirmed that the reaction proceeded as expected, and reactions, quenched by filtration, were subsequently lyophilized to remove water and buffer. Strata SCX columns were used to enrich the YwfG product from the crude reaction mixture. Columns were activated by washing with 1 mL of 1 M acetic acid, followed by 2 mL water. Reaction products from four YwfG reactions were dissolved in 500 μL water and run over the column. The column was washed with 3 mL water and eluted with 1 mL 97:3 water-ammonium hydroxide. Elution released the bound YwfG reaction product **7** and Phe. This sample was lyophilized, then dissolved in D_2O to permit NMR analysis. ^{1}H, gCOSY, HSQC, and gHMBC spectra were collected. LC/MS data was collected in positive ion mode.

RESULTS

Expression of BacABC and YwfGH in E. coli and Protein Purification

The five genes encoding BacABC and YwfGH were PCR amplified out of *B. subtilis* sp. 168 genomic DNA. The encoded proteins were expressed in *E. coli* with N-terminal His tags and purified through NiNTA affinity chromatography. Yields of each protein were: BacA – 12 mg/L, BacB – 26 mg/L, BacC – 37.5 mg/L, YwfG – 20 mg/L, YwfH – 20 mg/L. BacBC and YwfGH were purified to near homogeneity by NiNTA chromatography, while BacA required further purification by FPLC-based gel filtration (Figure 1b). BacB was found to be unstable without glycerol in storage buffer. To date no activity has been detected in assays with BacC, a putative nicotinamide-dependent reductase or dehydrogenase.

BacA Acts as a Novel Non-Aromatizing Prephenate Decarboxylase to Generate Dihydro-4-hydroxyphenylpyruvate Regioisomer 4, an A_{258} Species

Our first insight into the biosynthetic route to anticapsin came from the observation that incubation of prephenate with BacA led to the formation of a new product in a cofactor-independent manner. By analytical HPLC, we observed the disappearance of the prephenate peak and appearance of a new product peak with λ_{max} of 258 nm (ε = 2900 M^{-1} cm^{-1}) (SI Figure S1). The k_{cat} for BacA mediated conversion of prephenate to this A_{258} product is 190 min^{-1} with a K_m of 70 μM for prephenate (Figure 3).

In order to structurally characterize the product of the BacA reaction, large-scale reactions were run in D_2O and quenched at 2.5 hours, when formation of the A_{258} nm species was nearly complete, and ^{1}H, gCOSY and gHSQC NMR spectra of the reaction mixture were obtained. The ^{1}H NMR spectrum of the BacA reaction was compared to the ^{1}H NMR spectrum of prephenate. The spectrum of the prephenate starting material (Figure 2c) contains a multiplet at δ_H 4.50 ppm due to H_7 alpha to the alcohol. Its four olefinic protons are found as multiplets at δ_H 5.91 and 6.01. Protons H_3 are identified in a singlet at δ_H 3.12. By contrast, the ^{1}H NMR of the BacA reaction contains a new product, as well as residual prephenate and phenylpyruvate (PP) impurities. Three olefinic protons, one fewer than found in prephenate, are detected in the ^{1}H NMR spectrum (Figure 2d). Two of these protons give rise to a multiplet at δ_H 5.97 (H_5, H_6), while the other is observed at δ_H 5.73 (H_9). The proton alpha to the alcohol (H_7) is retained in the new product, though shifted upfield by ~0.25 ppm. The H_3 protons are retained

as well, though shifted downfield at δ_H 3.54 ppm. Appearance of a new aliphatic proton at δ_H 2.41 (H_8) is observed. gCOSY of the BacA product (spectrum in SI Figure S2) reveals coupling between H_8 and the proton alpha to the alcohol (H_7), as well as with H_9 at δ_H 5.73. H_7 is also found to couple to one of the olefinic protons in the δ_H 5.97 multiplet (H_5, H_6).

The data are all consistent with assignment of the new reaction product as H_2HPP **4**, a dihydro-4-hydroxyphenylpyruvate regioisomer. BacA catalyzes decarboxylation and protonation at $C_{6'}$, with a shift of the participating double bond from the $C_{5'\text{-}6'}$ position to the $C_{4\text{-}9}$ position. H_2HPP **4** still contains a cyclohexadienol moiety as found in prephenate, but with one of the double bonds rearranged positionally. In reactions performed in D_2O a deuteron is incorporated at C_8, leaving only one proton at that carbon to be observed by ^{1}H NMR. Full characterization of H_2HPP **4** was hampered by its tendency to rearrange to another H_2HPP isomer **5** as described below. However, enough H_2HPP **4** was present to allow for partial carbon shift assignment using gHSQC correlations (Table I, SI figure S3).

Rearrangement of 4 to 5, a conjugated H_2HPP regioisomer (A_{295}) species

In the BacA reaction mixtures subsequent slow conversion of H_2HPP **4** (λ_{max} = 258 nm) to a new product with absorbance maximum at 295 nm was detected ($\varepsilon = 15300 \pm 200\ M^{-1}\ cm^{-1}$). These observations are in accord with a recent paper from Rajavel et al. that appeared while this manuscript was in preparation (23). Rajavel et al. ascribed the slow A_{295} formation to an auto-oxidation. (We note below that we assign structures to the BacA and the BacB products that differ from those tentatively assigned by Rajavel et al.). After filtration of the BacA reactions to remove the protein we observed that the slow conversion of **4** (A_{258}) to **5** (A_{295}) (rate of approximately 0.15 μM min^{-1} in the filtered reaction buffer) was independent of the presence of BacA. We were able to complete a full proton and carbon NMR assignment of H_2HPP **5** and to establish its structure as a rearranged H_2HPP isomer in which the endocyclic olefin has migrated to the exocyclic position. The conjugation of the exocyclic double bond with both the $C_{5\text{-}6}$ olefin in the cyclohexene ring and with the C_2 keto group accounts for the longer wavelength absorbance maximum and the greater stability of the conjugated dienone system.

Both 1D- and 2D-NMR experiments, including ^{1}H, ^{13}C, gCOSY, gHSQC and gHMBC (Figure 2, SI Figures S5-S8, Table II), were performed to fully elucidate the structure of **5**. Comparison of the ^{1}H NMR spectra of prephenate, H_2HPP **4**, and the reaction mixture from lengthy overnight incubations of BacA and prephenate (Figure 2c, d, e) indicated that the BacA reaction that produced **4** was followed by nonenzymatic formation of **5**. Integrations of the olefinic proton multiplet in the spectrum of new product **5** (δ_H 6.26-6.34) indicated that the product has three olefinic protons (H_3, H_5, H_6). Additionally, retention of the H_7 proton alpha to the alcohol was observed, indicating that the alcohol functionality was preserved during this reaction. Another distinctive, new feature of compound **5** was its two diastereotopic methylene groups. 2D gCOSY showed a spin system with four distinct aliphatic protons at δ_H 1.59, 2.06, 2.59, and 3.17 (Protons H_{8a}, H_{8b}, H_{9a}, H_{9b}, respectively; Figure 2b). Two of the methylene protons, H_{8a} and H_{8b}, coupled to proton H_7 (δ_H 4.41-4.47) alpha to the alcohol. H_7 in turn coupled to one of the olefinic protons in the multiplet at δ_H 6.26-6.34 (H_6). This indicated that one of the cyclohexene olefins of H_2HPP **4** had been replaced by two methylene groups to form H_2HPP **5**. ^{13}C and heteronuclear 2D experiments further corroborated this structural assignment (spectra in SI Figures S5-S8). Two distinct carbonyl signals were observed in the ^{13}C NMR spectrum, one with a shift consistent with a carboxylic acid (δ_C 172.8), the other with a pyruvyl ketone (δ_C 195.7), indicating loss of one carboxylic acid from prephenate. Four distinct alkene carbons could be detected by ^{13}C NMR. Additionally, the signals corresponding to two aliphatic carbons (δ_C 24.23 and 30.5) and a carbon alpha to an alcohol group were

apparent (δ_C 65.74). gHMBC and gHSQC experiments allowed assignment of specific carbons to the peaks observed by ^{13}C NMR.

The mass of the reaction product H_2HPP **5** as determined by high resolution LC/MS ($C_9H_{10}O_4$ $[M\text{-}H]^-$ *m/z* 182.0588 (calc. *m/z* 182.0579)) is consistent with loss of CO_2 and net gain of a proton as in the NMR assignment of the structure.

To further evaluate the proposed BacA mechanism (Figure 2a) the reaction was carried out in deuterated water and monitored by ^1H NMR spectra every 6 minutes for 12 hours (Figure 3). Loss of the signals from prephenate (Pre) was observed, accompanied by the formation of H_2HPP **4**. At longer timepoints the proton signals from **4** decreased as **5** was formed by nonenzymatic rearrangement. In these conditions loss of a C_8 proton signal was observed, consistent with a proposed mechanism in which decarboxylation is followed by protonation (in these conditions, deuteration) at this position. Intriguingly, no deuterium incorporation was found at C_9, as would be initially expected for isomerization of the double bond into conjugation accompanied by protonation from solvent.

In sum, the initial BacA product was identified as 3-(4-hydroxycyclohexa-1,5-dienyl)-2-oxopropanoic acid, referred to as H_2HPP **4**. This compound could undergo a nonenzymatic isomerization to produce 3-(4-hydroxycyclohex-2-enylidene)-2-oxopropanoic acid, referred to as H_2HPP **5**.

BacB Catalyzes the Rapid Isomerization of 4 to 5

In accord with the observations of Rajavel et al. (23), we observed that BacB catalyzes the rapid conversion of the BacA product **4** to the same A_{295} product **5** (Figure 2e, f) obtained through nonenzymatic isomerization. For evidence of the identity of these products the reaction was monitored in real time by NMR (Figure 4d). In deuterated buffers BacB converts **4** to **5** with regioselective incorporation of one deuteron at C_9 (Figure 4c), consistent with a proposed mechanism in which C_3 of H_2HPP regioisomer **4** is deprotonated to the enolate anion and then the dienolate is reprotonated regiospecifically at C_9 to yield H_2HPP regiosomer **5.** High-resolution MS assigned a *m/z* of 182.059 ($C_9H_{10}O_4$ $[M\text{-}H]^-$ (calc. *m/z* 182.0579)) to the BacB product, which is identical to the mass of the non-enzymatically produced product. When the reaction was run in D_2O, the *m/z* was equal to 184.0684 ($C_9H_8D_2O_4$ [M*]– (calc. *m/z* 184.0705)), in accordance with double deuterium incorporation. These NMR and mass data lead us to confidently conclude that the same product H_2HPP **5** could be produced by nonenzymatic rearrangement of H_2HPP **4** or catalysis by BacB.

In kinetic studies in which both BacA and BacB were incubated with prephenate, H_2HPP **4** did not build up and rapid formation of **5** (λ_{max} = 295 nm) was observed (Figure 4b). We observed that the rate of **5** formation under co-incubation conditions was roughly equivalent to the rate of **4** formation when only BacA was included in the reaction, suggesting BacB catalyzes a very rapid isomerization. Rajavel et al. reported a k_{cat} of 1471 min^{-1} for this transformation (23).

Rajavel et al. ascribed the nonenzymatic conversion of the A_{258} to an A_{295} species as an auto-oxidation and proposed tentative assignments of structures (SI Figure S15), with only rudimentary ^1H NMR and no 2D or ^{13}C NMR experiments. They reported the product of the BacA reaction as 3-(4-hydroxycyclohexa-2,5-dienyl)-2-oxopropanoic acid, while the nonenzymatic auto-oxidation was suggested to involve oxidation of the C_7 alcohol to a ketone (23). We detect the C_7-proton in both H_2HPP isomers **4** and **5**, as well as extensive coupling between four distinct aliphatic protons in isomer **5** by gCOSY and ^1H NMR (Figure 2b, e), which strongly support our assignments of the two H_2HPP regioisomers. BacB thus acts as a

1,3-allylic isomerization catalyst, accelerating the thermodynamically favored (nonenzymatic) conversion of **4** to **5**, and reducing off pathway dehydration/aromatization to phenylpyruvate.

YwfH Catalyzes Conjugate Reduction of H_2HPP

Incubation of H_2HPP **5** accumulating from BacA/BacB action with purified YwfH and NADH led to loss of **5**, as monitored by analytical HPLC (Figure 5). No new UV-active product peak could be detected by HPLC, indicating disruption of the chromophore in H_2HPP **5**. Since the YwfH reaction was dependent on NADH we anticipated that hydride transfer to one of the electropositive centers in the conjugated dienone system of H_2HPP **5** had occured. NMR experiments were used to characterize the product of this reaction. However, interpretation of the spectra was hindered by the presence of NADH and NAD^+ at excess over H_2HPP **5** in the reaction. Loss of H_2HPP **5** and peaks attributed to a new product could be detected by ^{1}H NMR (SI Figure S10). gCOSY (SI Figure S11) data provided a tentative assignment of the YwfH product as 3-(4-hydroxycyclohex-2-enyl)-2-oxopropanoic acid, which we have termed H_4HPP (**6**) (tetrahydro-4-hydroxyphenylpyruvate). The product had a *m/z* of 184.073 ($C_9H_{12}O_4$ $[M-H]^-$ calc. *m/z* 184.0736), equivalent to a 2H addition to H_2HPP and consistent with a hydride-mediated reduction of C_4 using NADH and subsequent protonation of the enolate at C_3 (Scheme 2).

YwfG is an Aminotransferase that Converts H_4HPP (6) into Tetrahydrotyrosine (7)

We anticipated that if H_4HPP (**6**) could be converted to an amino acid it could be purified away from the nicotinamide cofactors that hindered complete NMR characterization. To this end the YwfH reaction mixture, containing H_4HPP (**6**), NADH (a co-substrate included in the reaction) and NAD^+ (a byproduct of the reaction) was incubated with the putative aminotransferase YwfG. When L-Phe was used as an amino donor co-substrate in the above reaction a new product peak was detected by analytical HPLC (Figure 5). This peak displayed the characteristic λ_{max} (338 nm) of amino acids derivatized with OPA. It was not observed when either H_2HPP isomer was used as a substrate. An ion exchange resin was used to separate Phe and this new amino acid product from the cofactors, H_4HPP (**6**), and phenylpyruvate (PP) coproduct. A combination of 1D- and 2D-NMR studies, including ^{1}H, gCOSY, gHSQC, and gHMBC, revealed the structure of the YwfG reaction product to be tetrahydrotyrosine **(7)** (H_4Tyr) (Scheme 2, Table III, SI Figure S12-S14). By ^{1}H NMR (Figure 6) it was found that the product had two olefinic protons (H_5 and H_6). In addition, retention of the H_7 proton, alpha to the alcohol, was observed. gCOSY data (SI Figure S12) showed an extensive spin system between the methylene protons (H_8 and H_9) and remaining olefinic protons (H_5 and H_6), as well as H_7, which is consistent with a cyclohexenyl ring. Appearance of an additional proton at δ_H 3.27 was indicative of amino acid formation. gHSQC and gHMBC correlations confirmed structural identification as well as allowed assignment of carbon shifts. The *m/z* of the compound $C_9H_{15}NO_3$ was determined by high resolution LC/MS as 185.1047 ($[M+Na]^+$ calc. *m/z* 185.1052). These experiments validate that YwfG is a transaminase and that it produces H_4Tyr (**7**), a novel metabolite for *B. subtilis*. In turn the H_4Tyr (**7**) structure provides further evidence that the YwfH product is H_4HPP (**6**), assuming the only role of YwfG is to reductively aminate the C_2 ketone of H_4HPP (**6**).

DISCUSSION

The antibiotic bacilysin exemplifies the biosynthetic strategy of packaging a toxic/reactive amino acid unit as part of an oligopeptide, here the dipeptide L-Ala-L-anticapsin (bacilysin), for uptake by a sensitive cell (12,13). Once internalized, the dipeptide is susceptible to peptidase action to release free anticapsin in the targeted cell (11,14). The warhead of anticapsin is the epoxycyclohexyl ketone which is believed to capture the reactive thiolate side chain

nucleophile in the active site of glucosamine-6-phosphate synthase, a key enzyme for cell wall assembly (14,15).

It had been shown that the epoxycyclohexanone scaffold of anticapsin is derived metabolically from prephenate (17) but the nature of the intermediates have not previously been defined. Genetic studies on bacilysin (Bac) production in *Bacillus subtilis* identified the importance of a five gene cluster *bacA-E (10).* A sixth gene, *ywfG*, is encoded in the cluster, though it seems over time to have escaped inclusion in the Bac biosynthetic annotation. A seventh gene, the adjacent *ywfH*, is immediately downstream of the *bac* genes and encoded in the opposite DNA strand from the upstream six. In this study we have overproduced the Bac enzymes believed to be involved in anticapsin biosynthesis (BacA, B, and C) as well as the YwfG and H proteins in *E. coli* to begin *in vitro* reconstitution studies of the antibiotic biosynthetic pathway.

At the outset of this work it was not clear if prephenate or arogenate (pretyrosine) was the substrate for initiation of the Bac pathway. In our initial set of assays both prephenate and arogenate were tested with the various permutations of the purified proteins and cofactors. No transformation of arogenate was detected in any combination but incubations containing BacA led to loss of prephenate, suggesting BacA catalyzes the first step in the pathway and that prephenate is the initial substrate.

Bioinformatic analysis indicates that BacA is a member of the prephenate dehydratase family of enzymes. Typically these enzymes decarboxylate prephenate with expulsion of the *para*-OH, aromatizing the cyclohexadienyl ring and yielding phenylpyruvate on the way to phenylalanine (Figure 7) (24,25). The common alternative route for prephenate processing that involves decarboxylation occurs with loss of the para-H substituent as a hydride ion to NAD^+ to yield 4-hydroxyphenylpyruvate as an immediate precursor to tyrosine (Figure 7) (24). In contrast, BacA decarboxylates prephenate without aromatization, using one of the olefins as a site for isomerization and net protonation at C_8. Presumably prephenate is oriented in the active site of BacA to allow an active site acid to deliver a proton to C_8 as the C_4-COO^- bond breaks. The initial product of such a decarboxylation/olefin isomerization (**4**) would still contain a cyclohexadienol moiety but with the double bond positionally rearranged from the starting prephenate molecule.

The nascent H_2HPP **4** product that accumulates from BacA is metastable and rearranges, in a process we have shown to be nonenzymatic, to H_2HPP isomer **5** which now has the diene conjugated to the C_2 ketone, accounting for the chromophore at 295 nM. We postulate the second isomerization is initiated by abstraction of an acidic α-keto proton at C_3, to generate a dienolate transition state (Scheme 3) that has carbanionic character both at C_3 and at C_9. Protonation at C_9 is clearly favored at equilibrium, both nonenzymatically and in the presence of BacB. BacB has recently been crystallized by Rajavel et al. (23) and shown to be a member of the bicupin family. The allylic isomerase activity of BacB is robust and at 1500 min^{-1} (23) is likely to be physiologically relevant. Perhaps enzymatic acceleration of the allylic isomerization by BacB, which moves one of the double bonds of the cyclohexadienol moiety of H_2HPP **4** from an endocyclic to a conjugated exocyclic position in H_2HPP **5**, may be suppressing unwanted intramolecular decomposition of **4** to phenylpyruvate.

The net result of these tandem BacA- and BacB-mediated transformations is two sequential migrations of a double bond in prephenate: first from the $C_{5'\text{-}6'}$ locus to the $C_{4\text{-}9}$ locus, subsequently from the $C_{4\text{-}9}$ locus to the $C_{3\text{-}4}$ locus (Figure 2a). The final position at $C_{3\text{-}4}$ is in conjugation with the original $C_{5\text{-}6}$ double bond from prephenate and the C_2 keto group, as CO_2 is released.

While this manuscript was in preparation a report from Rajavel et al. was published presenting the crystal structure of BacB and also a subset of kinetic studies: that BacA can convert

prephenate in two steps to a 293 nm absorbing product and that BacB can accelerate formation of the A_{293} absorbance. They ascribed the A_{293} material to be either an auto-oxidation of the BacA product or a catalyzed oxidation by BacB. We agree that BacB catalyzes conversion of the BacA product to a novel product, and that the BacA product converts to the identical product nonenzymatically, but disagree that this process is an oxidation. Conversion of **4** to **5** is instead an isomerization between two H_2HPP isomers. Rajavel et al. provided low resolution mass spec data that the BacA product (at 181.9) lost one hydrogen in proceeding to the BacB product (180.9). Some undeveloped proton NMR data was presented but no ^{13}C or 2D experiments reported. Their tentative conclusion was that the BacA product underwent decarboxylation and replacement of the carboxylate by a proton, yielding no change in the cyclohexadienol moiety of prephenate. They also concluded that BacB acted to convert the C_7 alcohol to the corresponding ketone (2-oxo-3-(4-oxocyclohexadienyl)-2-oxopropanoic acid; SI Figure S15). In contrast, we acquired full NMR data for the A_{295} product and show conclusively that C_7 remains in the starting alcohol oxidation state in both H_2HPP **4** and H_2HPP **5**. The A_{295} chromophore is explained by the conjugated dienylketone moiety in structure **5**. Further high resolution MS data (MW of 182.0588) accords with the calculated value for both H_2HPP isomers **4** and **5**.

The conjugated diene of the H_2HPP isomer **5** is then set up for a Michael type hydride addition to generate H_4HPP (**6**). Conjugate addition of the itinerant hydride to the C_4 end of the enone system and resultant protonation of the transient enolate at C_3 would saturate the exocyclic double bond in H_2HPP **5**. This is accomplished by YwfH utilizing NADH as hydride donor. YwfH action can be monitored by loss of the 295 nm chromophore in the H_2HPP **5** substrate although kinetics are complicated by the simultaneous redox change in the NADH cosubstrate.

To further characterize the skeleton of H_4HPP (**6**) we utilized the fourth enzyme YwfG, a predicted transaminase that sits next to BacE in the *Bacillus* genome, to convert the C_2 keto group of the YwfH product to a C_2 amino group, thereby creating a stable molecule that could be purified and analyzed. The resultant product, H_4Tyr (**7**), was characterized by MS and ^{1}H and 2D-NMR. Thus, the four enzymes BacA, BacB, YwfH, and YwfG act sequentially to convert prephenate to tetrahydrotyrosine.

It is possible that YwfG and YwfH should be renamed BacF and BacG, respectively, to correct confusing annotation, although we realize we have not established that these enzymes are on pathway to anticapsin in addition to H_4Tyr (**7**). Further work will determine whether such a name change is indeed appropriate.

In this regard, given that BacA, BacB, and YwfH convert prephenate to H_4HPP, the resultant scaffold is now set up for the three subsequent transformations needed to produce anticapsin: transamination at the C_2 keto group, epoxidation of the remaining C_5-C_6 double bond, and oxidation of the C_7 hydroxyl to the ketone (Scheme 4). It is not yet clear in which order those three steps occur. There are two remaining enzyme candidates: BacC, a predicted NAD(H)-dependent short chain oxidreductase; and YwfG, which we have shown to be a transaminase. If BacC converts the C_7-OH to the C_7-ketone found in anticapsin, the pathway would seem to be short one epoxidase. Our first expectation was that BacB might be such an oxygenation catalyst. Its x-ray structure shows metal binding in a dicupin fold (23) and thus might fall in the quercitinase family of oxidation enzymes. On the other hand Steinborn et al. (10) have suggested BacB has homology to isomerase and guanyltransferase members; indeed, the observed activity reported here is that of an allylic isomerase. Future experiments will address the metal content of BacB and whether it is capable of catalyzing epoxidation in addition to isomerization. In addition, further studies with BacC and BacB are required to determine if H_4HPP and/or H_4Tyr are directly on pathway to anticapsin.

What is firmly established from these *in vitro* studies with purified BacA, BacB, YwfG and YwfH is that these four enzymes can convert prephenate to tetrahydrotyrosine, a novel nonproteinogenic amino acid in the *Bacillus* metabolome (Scheme 4). It is likely this is the biosynthetic route used by cyanobacteria to construct this nonproteinogenic building block found in certain nonribosomal peptides. The stereochemistry of the tetrahydrotyrosine formed from BacA, BacB, YwfH, and YwfG action is yet to be fully determined. It is likely to be unchanged from prephenate at C_7, to be *S* at C_2 given the L-specificity of YwfG, but the C_4 stereochemistry remains at issue. In anticapsin the C_4 stereochemistry is *S*, so it is anticipated that YwfH will specifically produce this enantiomer if H_4Tyr is on the biosynthetic pathway. Validation of these predictions will require future comparison with synthetic standard H_4Tyr diastereomers.

Supplementary Material

Refer to Web version on PubMed Central for supplementary material.

Acknowledgments

We thank Drs. Laurence Davin and Norman Lewis for their gift of a sample of arogenate, and Emily Balskus, Leah Blasiak, and Elizabeth Sattely for helpful advice and discussions.

Abbreviations

B. subtilis	Bacillus subtilis
E. coli	Escherichia coli
Pdt	prephenate dehydratase
H_2HPP	dihydro-4-hydroxyphenylpyruvate
H_4HPP	tetrahydro-4-hydroxyphenylpyruvate
H_4Tyr	tetrahydrotyrosine
Pre	prephenate
NADH	nicotinamide adenine dinucleotide, reduced
NAD^+	nicotinamide adenine dinucleotide
PLP	pyridoxal 5′-phosphate
OPA	phthaldialdehyde
TEAA	triethylammonium acetate
PP	phenylpyruvate
IPTG	isopropyl-β-D-galactopyranoside
BSA	bovine serum albumin
NiNTA	nickel-nitrilotriacetic acid-agarose
SDS-PAGE	sodium dodecyl sulfate – polyacrylamide gel electrophoresis
LC-MS	liquid chromatography-mass spectrometry
NMR	nuclear magnetic resonance
gCOSY	gradient homonuclear correlation spectroscopy
gHSQC	gradient heteronuclear single quantum coherence

gHMBC	gradient heteronuclear multiple bond coherence
FPLC	fast protein liquid chromatography
HPLC	high-performance liquid chromatography
PCR	polymerase chain reaction
ORF	open reading frame

References

1. Stein T. Bacillus subtilis antibiotics: structures, syntheses and specific functions. Mol Microbiol 2005;56:845–857. [PubMed: 15853875]
2. Foster JW, Woodruff HB. Bacillin, a New Antibiotic Substance from a Soil Isolate of Bacillus subtilis. J Bacteriol 1946;51:363–369. [PubMed: 16561088]
3. Walker JE, Abraham EP. The structure of bacilysin and other products of Bacillus subtilis. Biochem J 1970;118:563–570. [PubMed: 4991476]
4. Baldwin JE, Adlington RM, Mitchell MB. Stereocontrolled enantiospecific synthesis of anticapsin: revison of the configuration. J. Chem. Soc., Chem. Commun 1993;17:1332–1335.
5. Wild H. Enantioselective Total Synthesis of the Antifungal Natural Products Chlorotetaine, Bacilysin, and Anticapsin and of Related Compounds: Revision of the Relative Configuration. J Org Chem 1994;59:2748–2761.
6. Atsumi K, Oiwa R, Omura S. Production of bacillin by Bacillus sp. strain no. KM-208 and its identity with tetaine (bacilysin). J Antibiot (Tokyo) 1975;28:77–78. [PubMed: 1126868]
7. Kaminski K, Sokolowska T. Letter: The probable identity of bacilysin and tetaine. J Antibiot (Tokyo) 1973;26:184–185. [PubMed: 4205876]
8. Krynski S, Borowski E, Kuchta A, Borowski J, Becla E. Studies on tetaine, a new antibiotic from theta strain of Bacillus pumilus. Biul Panstw Inst Med Morsk Trop J W Gdansku 1952;4:301–309. [PubMed: 13009425]
9. Loeffler W, J S-M, Tschen N, Vanittanakom M, Kugler E, Knorpp T-F, Hsieh T-G, Wu. Antifungal effects of bacilysin and fengymycin from *Bacillus subtilis* F-29-3: A comaprison with activities of other *bacillus* antibiotics. J. Phytopathology 1986;115:204–213.
10. Steinborn G, Hajirezaei MR, Hofemeister J. bac genes for recombinant bacilysin and anticapsin production in Bacillus host strains. Arch Microbiol 2005;183:71–79. [PubMed: 15609023]
11. Kenig M, Vandamme E, Abraham EP. The mode of action of bacilysin and anticapsin and biochemical properties of bacilysin-resistant mutants. J Gen Microbiol 1976;94:46–54. [PubMed: 819624]
12. Chmara H, Woynarowska B, Borowski E. Epoxypeptide antibiotic tetaine mimics peptides in transport to bacteria. J Antibiot (Tokyo) 1981;34:1608–1612. [PubMed: 7037722]
13. Perry D, Abraham EP. Transport and metabolism of bacilysin and other peptides by suspensions of Staphylococcus aureus. J Gen Microbiol 1979;115:213–221. [PubMed: 528972]
14. Chmara H. Inhibition of glucosamine synthase by bacilysin and anticapsin. J Gen Microbiol 1985;131:265–271. [PubMed: 3884731]
15. Chmara H, Zahner H, Borowski E. Anticapsin, an active-site directed irreversible inhibitor of glucosamine-6-phosphate synthetase from Escherichia coli. J Antibiot (Tokyo) 1984;37:1038–1043. [PubMed: 6389459]
16. Roscoe J, Abraham EP. Experiments relating to the biosynthesis of bacilysin. Biochem J 1966;99:793–800. [PubMed: 4960795]
17. Hilton MD, Alaeddinoglu NG, Demain AL. Synthesis of bacilysin by Bacillus subtilis branches from prephenate of the aromatic amino acid pathway. J Bacteriol 1988;170:482–484. [PubMed: 3121591]
18. Inaoka T, Takahashi K, Ohnishi-Kameyama M, Yoshida M, Ochi K. Guanine nucleotides guanosine 5′-diphosphate 3′-diphosphate and GTP co-operatively regulate the production of an antibiotic bacilysin in Bacillus subtilis. J Biol Chem 2003;278:2169–2176. [PubMed: 12372825]

19. Tabata K, Ikeda H, Hashimoto S. ywfE in Bacillus subtilis codes for a novel enzyme, L-amino acid ligase. J Bacteriol 2005;187:5195–5202. [PubMed: 16030213]

20. Schmit JC, Zalkin H. Chorismate mutase-prephenate dehydratase. Partial purification and properties of the enzyme from Salmonella typhimurium. Biochemistry 1969;8:174–181. [PubMed: 4887851]

21. Dopheide TA, Crewther P, Davidson BE. Chorismate mutase-prephenate dehydratase from Escherichia coli K-12. II. Kinetic properties. J Biol Chem 1972;247:4447–4452. [PubMed: 4261395]

22. Nishioka, L. a. T. W. Improved assay for phenylpyruvic acid. Analytical Biochemistry 1972;45:617–623. [PubMed: 5060610]

23. Rajavel M, Mitra A, Gopal B. Role of Bacillus subtilis BacB in the synthesis of bacilysin. J Biol Chem 2009;284:31882–31892. [PubMed: 19776011]

24. Hermes JD, Tipton PA, Fisher MA, O'Leary MH, Morrison JF, Cleland WW. Mechanisms of enzymatic and acid-catalyzed decarboxylations of prephenate. Biochemistry 1984;23:6263–6275. [PubMed: 6395898]

25. Kleeb AC, Kast P, Hilvert D. A monofunctional and thermostable prephenate dehydratase from the archaeon Methanocaldococcus jannaschii. Biochemistry 2006;45:14101–14110. [PubMed: 17115705]

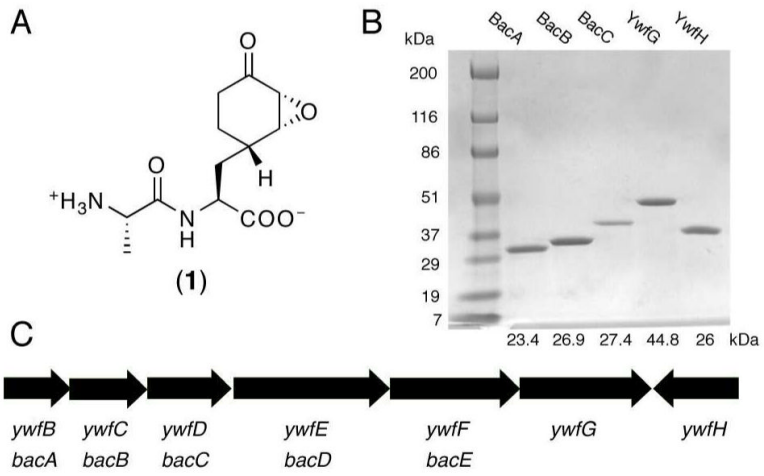

Figure 1.

A) Bacilysin (**1**). Anticapsin is the C-terminal amino acid. B) SDS-PAGE of purified BacA, B, C and YwfG, H. C) Bacilysin gene cluster (6688 bp). Designation of the genes has been historically confusing. The cluster was originally annotated as *ywfBCDEFGH*, however once genes *ywfBCDEF* were found to be relevant to the biosynthesis of bacilysin they were renamed *bacABCDE*. This work finds that *ywfGH* are likely relevant to bacilysin biosynthesis as well. Throughout the course of this paper proteins encoded by *ywfBCDEF* (*bacABCDE*) will be referred to as BacABCDE, while *ywfGH* protein products will be called YwfGH.

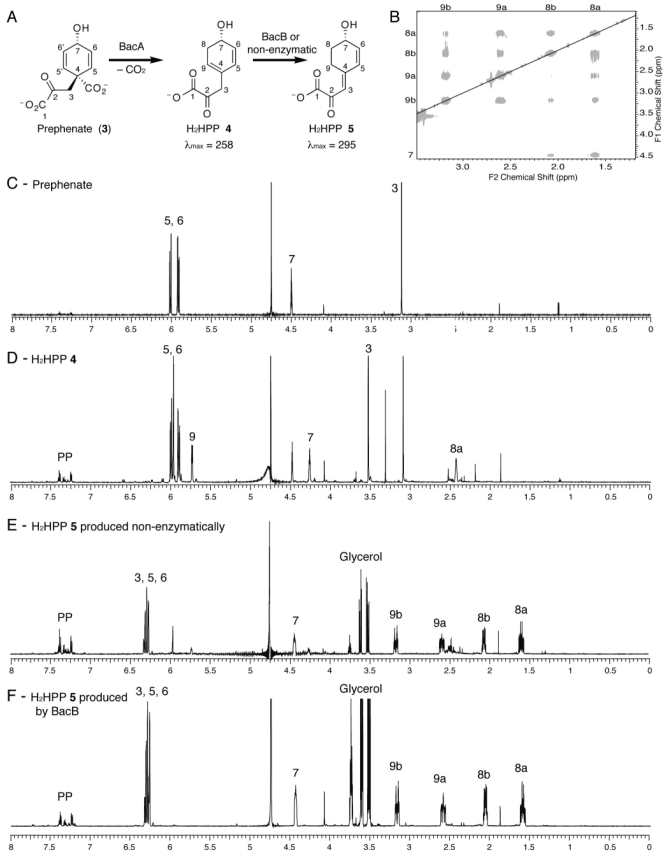

Figure 2.

A) BacA converts prephenate to H_2HPP **4**. H_2HPP **4** non-enzymatically isomerizes to H_2HPP **5**, or this isomerization can be catalyzed by BacB. B) gCOSY of the aliphatic region of H_2HPP **5**. C) ^{1}H NMR of prephenate in D_2O. D) ^{1}H NMR of H_2HPP **4** produced in D_2O by BacA (presaturation conditions used in NMR). E) ^{1}H NMR of H_2HPP **5** produced non-enzymatically from H_2HPP **4**. F) ^{1}H NMR of H_2HPP **5** produced from prephenate by BacA and BacB.

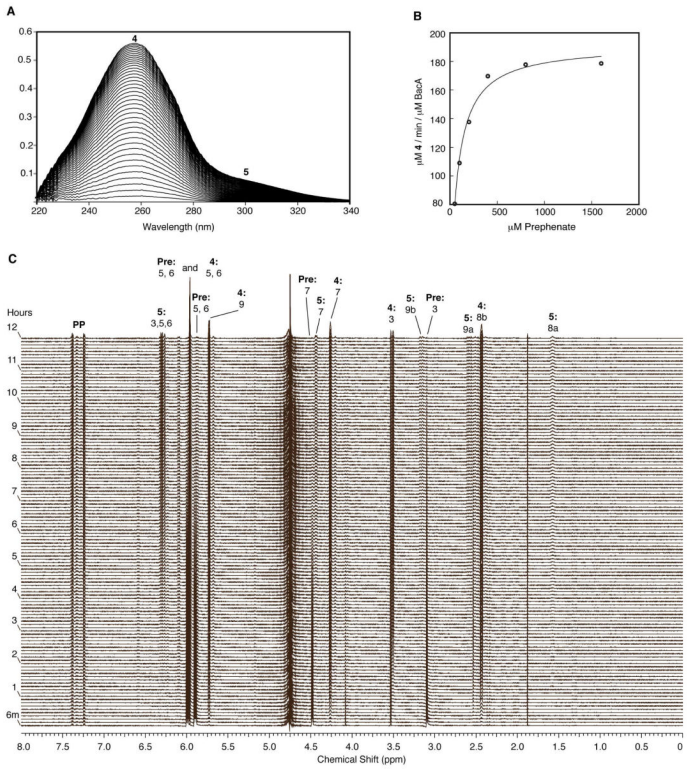

Figure 3.

A) Reaction of BacA and prephenate, scans taken every 30 seconds. B) Kinetics of BacA. C) Real-time NMR analysis of the BacA reaction. Prephenate (Pre) is converted to H_2HPP **4** rapidly, as observed in the disappearance of the prephenate $H_{5\text{-}6}$ and H_3 proton peaks and appearance of H_2HPP **4** proton peaks (H_7, H_9, for example). H_2HPP **4** disappears slowly as H_2HPP **5** is produced non-enzymatically (best seen with H_2HPP **5** methylene protons H_{8a}, H_{9b} and olefinic protons $H_{3,\,5,\,6}$).

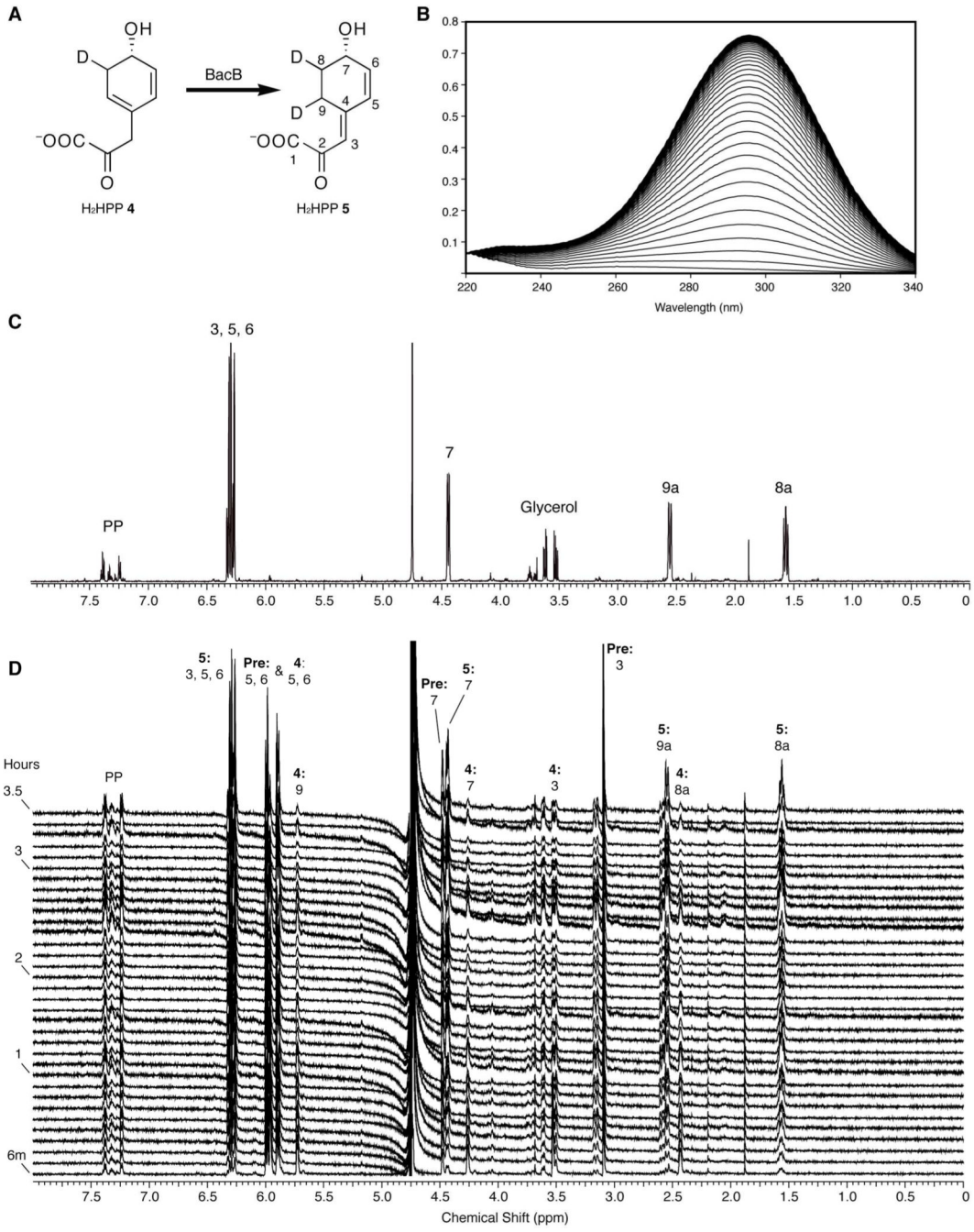

Figure 4.

A) Reaction catalyzed by BacB in D_2O. Deuterated H_2HPP **4** is produced by a BacA reaction run in D_2O. B) UV scans of a reaction including 100 nM BacA, 100 nM BacB, and 50 μM prephenate. Scans were taken every 30 seconds. C) ^1H NMR of the BacA-B product formed by co-incubation of prephenate in D_2O with both BacA and BacB. D) ^1H NMR scans of the BacB reaction in D_2O (spectra collected every 6 minutes for 3.5 hours). H_2HPP **4** disappears over the timecourse, as best seen with protons H_9 and H_7. H_2HPP **5** grows in (H_{8a} and H_{9a} for example).

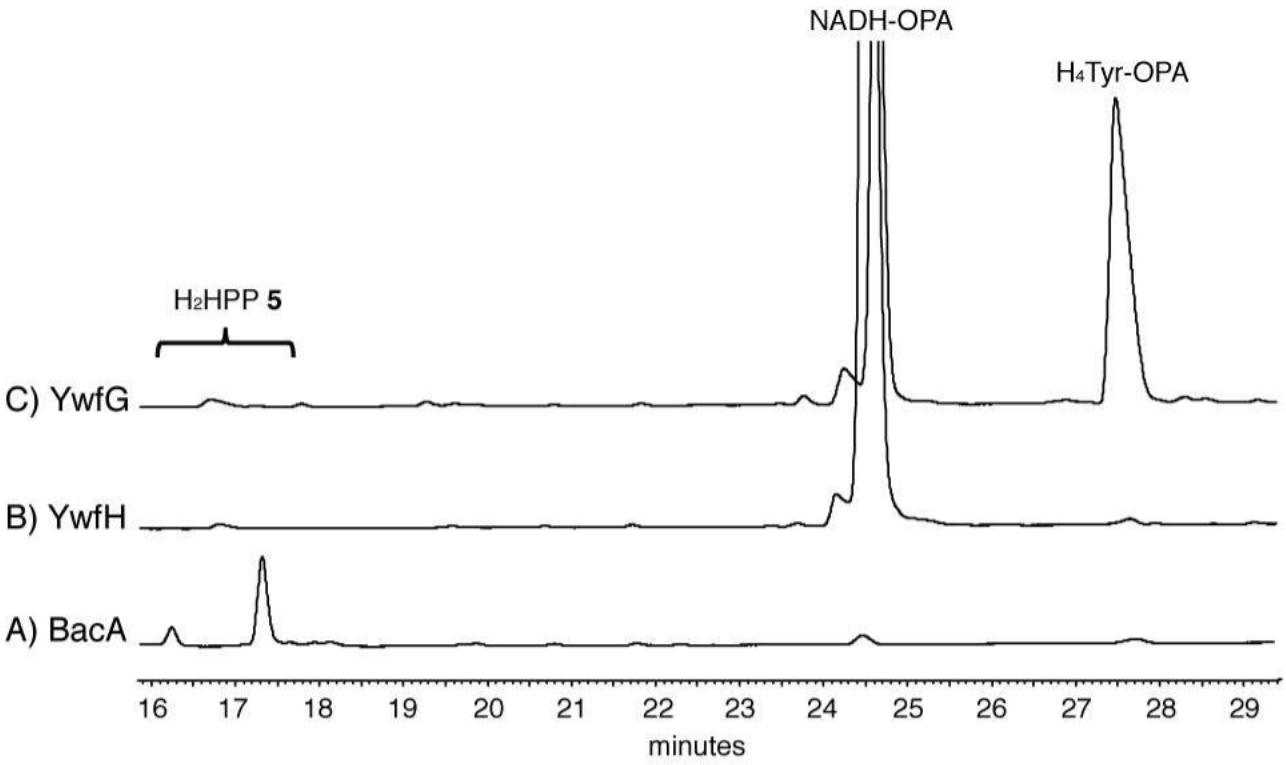

Figure 5.

HPLC Analysis of BacA, YwfH and YwfG Reactions. Samples above are from large-scale NMR reactions and monitored at 338 nm. A) H_2HPP **5**, produced by nonenzymatic isomerization of the BacA product H_2HPP **4**. B) When this product was incubated with YwfH and NADH disappearance of the H_2HPP **5** peak was observed. H_4HPP (**6**), the product of this reaction, has no chromophore and is not easily observed by HPLC. C) YwfG converted H_4HPP (**6**), a keto-acid, to H_4Tyr (**7**), an amino acid, when Phe was used as an amino donor. Primary amine containing compounds in the reactions were derivatized with OPA.

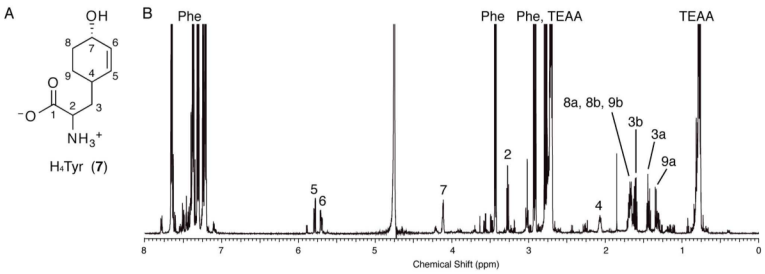

Figure 6.
NMR analysis of YwfG Reaction. A) H_4Tyr (**7**) B) ^{1}H-NMR of H_4Tyr, Phe and TEAA in D_2O.

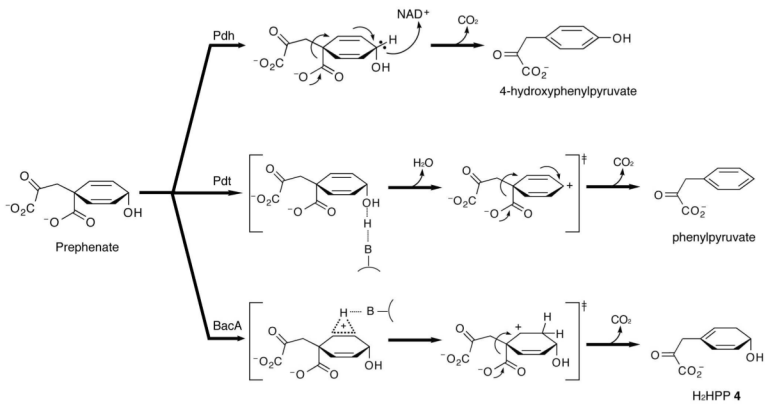

Figure 7.
Comparison of canonical prephenate dehydrogenase (Pdh) and prephenate dehydratase (Pdt) mechanism with proposed BacA mechanism.

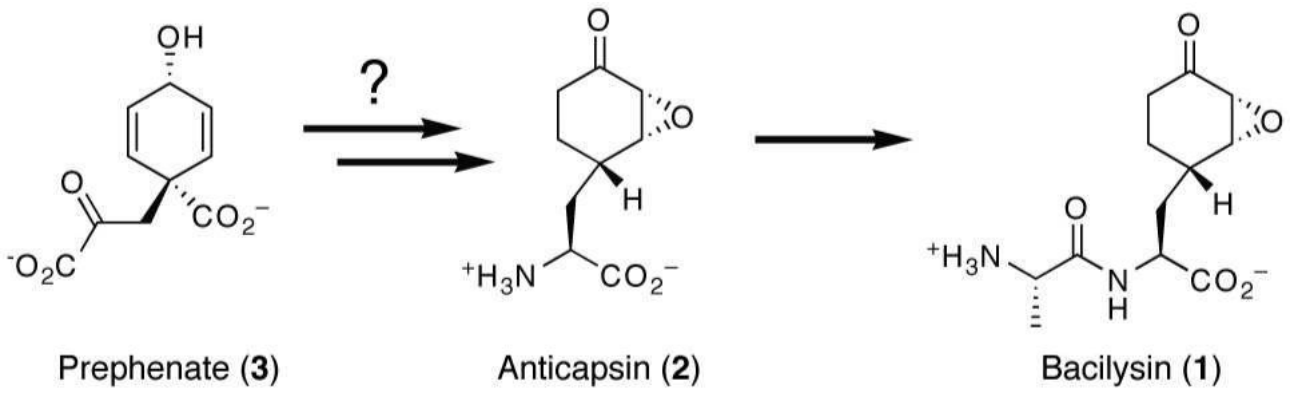

Scheme 1.
Prephenate (**3**) is the suspected precursor to anticapsin (**2**), which is ligated to alanine to produce bacilysin (**1**).

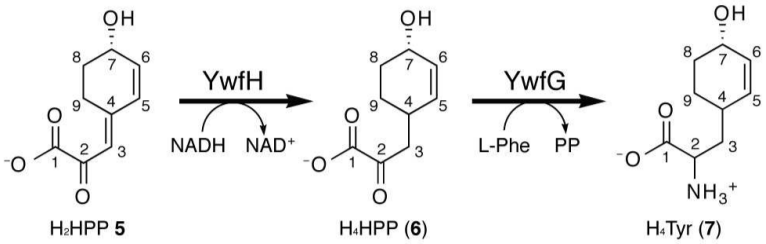

Scheme 2.

H_2HPP **5** conversion to H_4Tyr (**7**) by sequential YwfH and YwfG action.

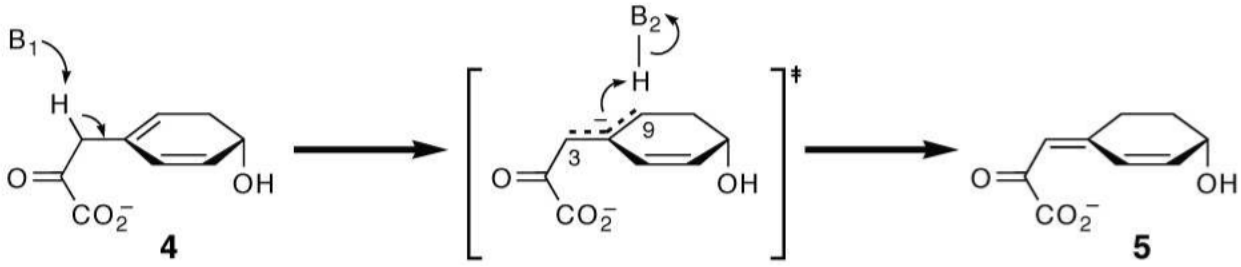

Scheme 3.
Conversion of H_2HPP **4** to H_2HPP **5** by BacB.

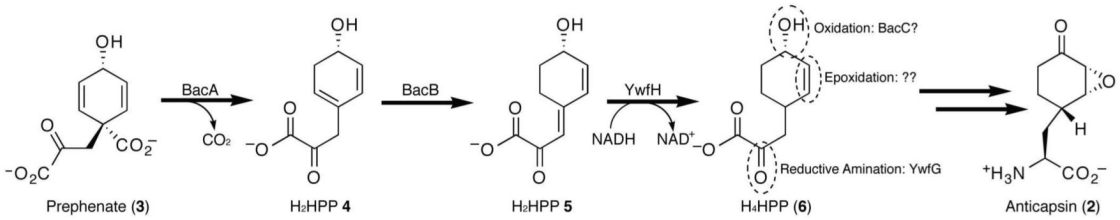

Scheme 4.
Possible Route to Anticapsin.

Table I

NMR Data for H_2HPP **4** produced in D_2O

	$^{13}C^{a}$ ppm	**^{1}H ppm, mult. (Hz)**	**gCOSY**
3	45.27	3.54, s	
5	128.59	5.97, m	
6	127.01	5.97, m	7
7	62.02	4.27, br. s.	6, 8
8	31.32	2.44, br. s.	7, 9
9	125.37	5.73, d (5.3)	8

[a]Carbon shifts assigned by gHSQC.

Table II

NMR data for H_2HPP **5** in D_2O

	$^{13}C^a$ ppm	^1H ppm, mult. (Hz)	gCOSY	gHMBC
1	172.8			
2	195.7			
3	136.46[b]	6.26-6.34, m	9a, 9b	1, 2, 3, 4, 5, 7, 8, 9
4	156.3			
5	121.11[b]	6.26-6.34, m	9a, 9b	1, 2, 3, 4, 5, 7, 8, 9
6	142.62[b]	6.26-6.34, m	7	1, 2, 3, 4, 5, 7, 8, 9
7	65.74	4.41-4.47, m	3/5/6[c], 8a, 8b	
8a	30.5	1.59, dddd (12.8, 11.7, 8.7, 4.5)	7, 8b, 9a, 9b	4, 7, 9
8b		2.06, dddd (12.8, 5.0, 5.0, 4.7)	7, 8a, 9a, 9b	4, 6, 7, 9
9a	24.23	2.59, dddd (17.4, 11.7, 4.7, 2.3)	3/5/6[c], 8a, 8b, 9b	4, 5, 7, 8
9b		3.17, ddd (17.4, 5.0, 4.7)	8a, 8b, 9a	3, 4, 5, 7, 8

[a] Carbon shifts assigned by ^{13}C NMR.

[b] Assigned to specific carbons using HSQC and HMBC.

[c] Olefinic protons 3, 5, and 6 could not be distinguished, as such gCOSY and HMBC correlations could not be specifically assigned to one proton.

Table III

NMR Spectral data for H_4Tyr (**7**) in D_2O

	^{13}C[a] ppm	^{1}H ppm, mult. (Hz)	gCOSY	gHMBC
1	184.25			
2	53.87	3.273, dd (7.5, 6.7)	3a, 3b	1, 3, 4
3a	40.95	1.439, ddd (13.7, 7.5, 7.5)	2, 3b, 4	1, 2, 4, 5, 9
3b		1.61, ddd (13.8, 13.8, 6.7)	2, 3a	1, 2, 4, 5, 9
4	31.66	2.067, m	9a	
5	135.49	5.778, dd (10.1, 2.8)	4, 6	3, 4, 7, 9
6	128.19	5.703, ddd (10.2, 3.5, 2.3)	4, 5, 7	4, 7, 8
7	64.28	4.119, m	6, 8a/8b/9a[b]	
8a	28.99	1.679, m	4, 7, 9a	4, 5, 6, 7, 8,
				9[b]
8b		1.679, m	4, 7, 9a	4, 5, 6, 7, 8,
				9[b]
9a	23.69	1.328, m	4, 8a/8b/9a[b]	3, 4, 7, 5, 8
9b		1.679, ma	4, 7, 9a	4, 5, 6, 7, 8, 9[b]

[a] Carbon shifts assigned by HSQC and HMBC.

[b] Aliphatic protons 8a, 8b, and 9b could not be distinguished, as such gCOSY and gHMBC correlations could not be specifically assigned to one proton.